Research Article

Mária Porubská*, Klaudia Jomová, Ľubomír Lapčík, and Jana Braniša

Radiation-modified wool for adsorption of redox metals and potentially for nanoparticles

Abstract: Electron beam irradiated sheep wool with absorbed radiation doses ranging from 0 to 165 kGy showed good adsorption properties toward copper cations. The Cu(II) being Lewis acid generated several types of complex salts based on carboxylates or cysteinates with ligands available in keratin. Under these conditions, cross-links were formed between the keratin chains. Experimental data obtained from Cu(II) adsorption using the concentration of 800–5,000 mg/L were tested for fitting to 10 isotherm models. Various compositions and architectures of the Cu(II)-complexes were specified to be responsible for different isotherm model fittings. The copper cation showed adherence to Langmuir, Flory–Huggins, and partially Redlich–Peterson models. The latter clearly distinguished the native wool from the modified ones. Another aim is to investigate the conditions for the adsorption of anti-microbial nanoparticles in addition to the redox-active metals on radiation-modified wool taking into account that the diffusion of nanoparticles into the modified wool is governed by electrostatic interactions.

Keywords: sheep wool, electron beam irradiation, adsorption, copper(II), isotherm model, fitting, nanoparticles

* **Corresponding author: Mária Porubská,** Department of Chemistry, Faculty of Natural Sciences, Constantine the Philosopher University in Nitra, 949 74 Nitra, Slovakia, e-mail: mporubska@ukf.sk
Klaudia Jomová, Jana Braniša: Department of Chemistry, Faculty of Natural Sciences, Constantine the Philosopher University in Nitra, 949 74 Nitra, Slovakia
Ľubomír Lapčík: Department of Physical Chemistry, Faculty of Science, Palacky University in Olomouc, 17. Listopadu 12, 771 46 Olomouc, Czech Republic; Institute of Food Technology, Faculty of Technology, Tomas Bata University in Zlin, Nam. T.G. Masaryka 5555, 760 01 Zlin, Czech Republic

1 Introduction

Contemporary nanotechnologies facilitate solutions of many environmental problems caused by irresponsible management of chemical processes. Carbon being in several modifications is utilizable for various purposes [1]. Carbon nanotubes show effective adsorption of heavy metals such as lead(II) [2]. Also, modified silica microspheres remove lead(II) from solutions [3] with the help of their large surface area.

Biopolymers such as keratin can also prove a good service for the removal of unwanted pollutants from the environment. Keratin properties, relevant composites, and use are presented in the book by Reddy et al. [4]. The search for effective use of excessive sheep wool is reflected in scientific studies dealing with the wool as a natural adsorbent. The essential component of wool, keratin, contains several types of functional groups capable to operate as binding sites for several species. The major metal-binding sites in wool are the carboxylic side chain groups and the sulfonate groups are minor binding site contributor [5]. That is why adsorption of metal cations is reported in several papers [6–8]. However, anion removal is also examined [9–12]. All the authors applied the adsorbate concentrations under 10 mmol/L probably because the increasing concentration decreases the removal percentage.

Besides inorganic pollutants, the removal of organic constituents as oil was also studied [13,14]. Wool was examined for adsorption of environmental tobacco smoke [15] and absorption of formaldehyde emitted from household products such as furniture [16].

The effort to improve the wool adsorptivity leads to the treatment of the wool surface using several ways. All chemical modifications [8,17–19] require wet processes, more operations and produce wastewater containing chemicals.

Application of corona or plasma represents a physical–chemical treatment of wool surface. Scales on the fibre surface serve as a barrier for diffusion processes, which adversely affects the sorption behaviour. However, the plasma treatment shows a descaling effect similar to the

chemical effect [20]. Some studies applying for corona show, besides others, that content of the positive charged functional groups is higher in the corona-treated wool fabrics in comparison with the untreated ones [21]. Hydrophilicity as well as dyeing properties are improved [22]. The better hydrophilicity, dyeability, antimicrobial and shrink proofing properties of wool fibres are also obtained using synthesis of silver nanoparticles on the fibres [23–25]. Enhancement deposition of titanium dioxide nanoparticles on wool/PET fabric is also supported by plasma pretreatment [25].

Recently, a modification of wool through the irradiation by accelerated electron beam affecting whole fibre volume was developed [26]. The significance of such a treatment lies mainly in the fact that it is an environmentally friendly, one-step, dry process without chemicals and wastewater. In addition, neither plasma nor corona treatment is feasible on an industrial scale, unlike electron irradiation. The dependence of physical–chemical properties of the electron-modified wool on absorbed dose as well as sorption of some metal cations are examined [26–29]. The actual results show enhancement of the metals sorption. However, several other useful effects can be expected. The electron radiation affects the zero charge point of the wool following absorbed dose [30]. Taking into account that charge of nanoparticles is important to maintain their stability as dispersion [31], modification of the zero charge point using the irradiation opens a way to modify the dispersion stability and subsequently an antimicrobial potential. So an appropriate combination of the good sorption properties of the irradiated wool and the antimicrobial effect using nanoparticle deposition seems to be an attractive idea. However, such projects need several research phases. The aim of this study is to examine the first step and that is sorption characteristics of Cu(II) on the electron irradiated wool with respect to models of selected adsorption isotherms.

Although other reporting researchers apply low adsorbate concentrations almost exclusively, when fitting some isotherm model is not too difficult, we also dealt with adsorbates of higher concentrations. The reason is that circular economy, besides others, should be focused on the recuperation of valuable components from various technological wastes containing a variable amount of the recyclable ingredients. In addition, they can be bacterially contaminated.

Applying higher Cu(II) concentrations in the range of about 800–5,000 mg/L (12.5–80 mmol/L) under adsorption on the electron-irradiated wool with various absorbed doses, we observed unexpected results showing extremes [32]. Till this time, any similar fact is not described in

scientific sources. Hence, 10 isotherm models are tested for the mentioned phenomenon and the results obtained are confronted with previous findings.

2 Materials and methods

2.1 Materials

Copper(II) sulphate pentahydrate $CuSO_4 \cdot 5H_2O$ p.a. was supplied by Centralchem, Slovakia. Testing solutions in the range of 12.5–80 mmol/L for the sorption experiments were prepared by diluting the corresponding stock solution with demineralized water.

The sheep wool came from spring sheep-shearing of a Tsigai–Suffolk crossbreed bred in Middle Slovakia. The samples were taken from various sites randomly and the fibre thickness was in the range of 27–33 μm.

2.2 Sheep wool scouring and irradiation

After removing the wool crude impurities manually, the wool was scoured repeatedly in warmish tap water until the rinse water was clean. An ultrasonic bath of 5 L in volume was used for the finish scouring so that about 12 g of wool put in a netted pouch was washed in 40°C tap water in the bath during a 10 min period. Then the water was exchanged and the washing was repeated. Finally, the wool was rinsed with 5 L of demineralized water. After the pouch was removed, and the trapped water ran off, the sample was dried in a laboratory oven at 40°C for 24 h. Such dried wool was stored under routine laboratory conditions. The samples put in separate unsealed polyethylene pouches and placed into carton boxes were irradiated in linear electron accelerator UELR-5-1S (Petersburg, Russia) of Progresa Final SK operator. The process parameters were as follows: installed energy of 5 MeV, intensity of 200 μA, mean power of 1 kW and mean dose rate of 750 kGy/h. The doses applied were 0–20–24–48–100–165 kGy repeating 100 kGy cycles plus needed supplementing dose, if necessary. Between individual irradiation cycles, the samples were allowed to cool down for 30 min to maintain a temperature below 50°C. The absorbed doses were checked dosimetrically. After being irradiated the samples were kept under usual laboratory conditions.

2.3 Electron microscopy

Scanning electron microscopy (SEM) images of the scoured wool fibres were taken by electron microscope Hitachi 6600 FEG (Japan) operating in the secondary electron mode and using an accelerating voltage of 1 kV [33].

2.4 Batch sorption experiments

The sorption experiments were conducted with Cu(II) solutions applying concentrations in the range of 12.5–80 mmol Cu/L (794–5,080 mg/L). The duration of 24 h contact of Cu(II) with wool was experimentally determined to be optimal. After being cut to 3–5 mm, the wool fibres of 0.2 g were placed into a small glass cup with a cap and the testing solution of 12 cm^3 in volume was added. Thorough wetting of the wool was ensured immersing it into the solution using a glass rod. The content of the glass cup was shaken for the first 6 h at room temperature on a laboratory horizontal shaker (TE, Kavalier, Czech Republic) and then kept in static mode for next 18 h. Then the remaining solution was filtered through KA5 filter paper and used for determination of residual Cu(II). Every sorption experiment was carried out in triplet. The sorptivity was calculated using the following equation:

$$S = (x_1 - x_2)/m \tag{1}$$

where S is the sorptivity defined as the mass of sorbate in mg per 1 g of the sorbent for individual wool samples when the particular testing solution is applied in specified concentration, x_1 is the mass of the Cu(II) added in the initial solution (mg), x_2 is the residual mass of the Cu(II) in the solution after selected contact period with the wool sample (mg) and m is the mass of wool sample taken for analysis (g). If x_2 is the residual Cu(II) mass at the equilibrium, then $S = q_e$.

2.5 Determination of residual Cu(II) concentration

The residual Cu(II) concentrations in the bath were determined using visible spectrometry (Specord 50 Plus, Analytikjena, Germany) with 1 cm cell recording spectrum within (450–1,000) nm. The selected range of the concentration in the bath was limited by the absorbance for the equilibrium concentration so that the read absorbance for $\lambda_{max} = 809$ nm was as accurate as possible and did not

exceed the value of 1.0. The spectrum was taken from the filtered bath and Cu(II) content was determined using relevant calibration curve. Concerning the spectra, the blank was the water extract obtained from the corresponding wool sample under identical conditions, however, without Cu(II). Under these conditions, the relative deviation did not exceed 5%.

2.6 Design of isotherms

Without any previously published information, we selected a set of 10 adsorption models assuming that they could include a fitting model. The data needed to calculate the parameters of the individual isotherm models were obtained from the graph dependencies generated for each model and absorbed dose using Excel, also providing correlation equations for linearized relationships. An overview of the conditions is given in Table 1.

3 Results and discussion

3.1 Characteristics of irradiated wool and copper complexes

Keratin is a fibrous structural protein-containing carboxyl groups in branches available to form related salts through ion exchanging mechanism. Since Cu(II) cation is Lewis acids, related Cu-salts readily coordinate with free electron pairs of amino-, imino- and hydroxyl functional groups abundantly present in the side branches. Accelerated electron beam splits disulphide bridges RS–SR linking stabilizing the main protein chains. The generated free RS˙ radicals are oxidized in the air giving cystine mono oxide R–S–SO, cystine dioxide R–S–SO$_2$, cysteine sulfonate (Bunte salt) R–S–SO$_3^-$, and these all are transformed into cysteic acid R–SO$_3$H step by step [26,27]. The main reaction pathway of radiation-damaged disulphide bonds involves one electron addition that yields the radical anion (SS˙$^-$) according to the reaction:

$$-CH_2-S-S-CH_2- \xrightarrow{e^-} -CH_2-\overset{\ominus}{S}-\overset{\cdot}{S}-CH_2- \tag{2}$$
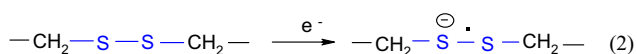
The unpaired electron in SS˙$^-$ resides in a three – electron σ – bond. Generally, radical anion SS˙$^-$ is highly

Table 1: The conditions of calculation and plotting curves to test fit of selected isotherm models (Meaning of basic symbols: C_e is concentration of adsorbate at equilibrium, q_e is amount of adsorbate adsorbed at equilibrium, C_0 is adsorbate initial concentration, Θ is degree of surface coverage; other appearing symbols belong to individual constants or indicators.)

No. (C_0, C_e; q_e; Θ)	Isotherm model	Units used for calculation	Plot of dependence
1	Langmuir	mg/L; mg/g	C_e against C_e/q_e
2	Freundlich	mg/L; mg/g	$\log C_e$ against $\log q_e$
3	Dubinin–Radushkevich	mg/L; mg/g	ε^2 against $\ln q_e$
4	Temkin	mg/L; mg/g	$\ln C_e$ against q_e
5	Flory–Huggins	mol/L; mol/g	$\log(1 - \Theta)$ against $\log(\Theta/C_0)$
6	Halsey	mg/L; mg/g	$\ln C_e$ against $\ln q_e$
7	Harkins-Jura	mg/L; mg/g	$\log C_e$ against $1/q_e^2$
8	Jovanovic	mg/L; mg/g	C_e against $\ln q_e$
9	Elovich	mg/L; mg/g	q_e against $\ln(q_e/C_e)$
10	Redlich–Peterson	mg/L; mg/g	$\ln C_e$ against $\ln(C_e/q_e)$

reactive, and in the oxygenated environment, it may react with dioxygen leading to the S-sulphonate (Bunte salt) up-to cysteic acid formation according to the reaction (3):

$$ (3) $$
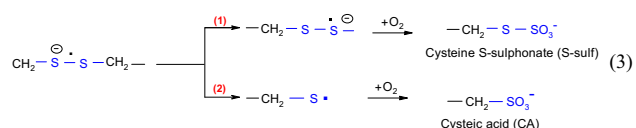
So, unlike native wool, in modified wool the number of acidic groups increases. Thereby besides carboxylates R-COO⁻, cysteinates are also formed. Depending on the different structure of both types of the salts, various complexes with own architectonic design have to be generated. Therefore, it should not be surprising that the formation of the complexes on the wool surface or in bulk plays important, if not determining, role. This also indicates the course of sorptivity for Cu(ɪɪ) on the different dosed wool (Figure 1), which shows atypical fluctuation in the range of the applied concentrations. Indeed, the formation of the Cu(ɪɪ) complexes with wool was proven using FTIR and ATR spectroscopy [32]. As found, Cu(ɪɪ) complexes often exhibit a distorted tetrahedral or octahedral structure [34]. Pentacoordinate copper(ɪɪ) complexes are more rarely encountered. In this case, the Cu(ɪɪ) coordination polyhedron is a square pyramid or less frequently a trigonal bipyramid. Based on the observed EPR spectra (*g*-factors), it was concluded that the coordination environment around copper(ɪɪ) ion is distorted octahedral or tetrahedral. From the shape of the EPR spectra, the formation of dimeric, tetrameric or polymeric structures cannot be excluded, most probably formed via carboxylate bridges [35,36]. The ligands coming from different keratin chains cause a crosslinking and, following the corresponding Cu(ɪɪ)-complex architecture, they act to

be larger or smaller barriers for the next diffusion of the cations into the fibre bulk. The type of generated Cu-complex on the wool surface or bulk is determined by Cu(ɪɪ) concentration, amount of acid groups, available ligands and steric possibilities. The diversity of these conditions is projected in the sorptivity fluctuation (Figure 1) except 24 kGy dosed sample. Since close 20 kGy dose also shows fluctuation, the 24 kGy dose may be critical with respect to the cleavage of −S−S− bonds to form cystine monoxide, cystine dioxide and primarily cysteine S-sulfonate (Bunte salt) [26]. This assumption will need to be further examined.

The similar dependences using equilibrium concentration C_e instead initial one C_0 cannot be displayed in one plot for all doses; however, differences between them can be seen from the dependences of C_e on C_0. As results from Table 2, all doses show strictly linear courses of the function differing in the position of the intersection with
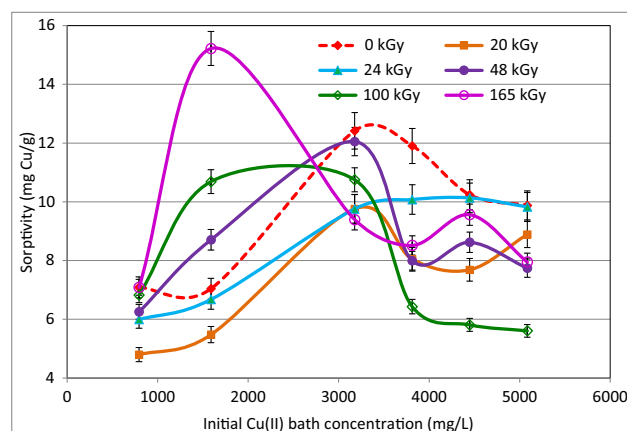

Figure 1: Sorptivity of Cu(ɪɪ) on wool native and electron irradiated with various absorbed doses.

Table 2: Characterization of adsorption curve shifts compared with the curves in Figure 1 using plot of $C_e = f(C_0)$

Dose (kGy)	$C_e = f(C_0) \rightarrow y = ax + b$	Correlation
0	$y = 0.9907x - 68.322$	$R^2 = 0.9999$
20	$y = 0.9907x - 45.147$	$R^2 = 1$
24	$y = 0.9895x - 54.442$	$R^2 = 1$
48	$y = 0.9975x - 77.853$	$R^2 = 0.9999$
100	$y = 1.0071x - 99.309$	$R^2 = 0.9998$
165	$y = 1.0049x - 111.73$	$R^2 = 0.9997$

the y-axis only. This shift gives the mutual position of the curves with the same doses if a common graph of the $q_e = f(C_e)$ function is constructed for all absorbed doses. The equation term b indicates the Cu(II) removing from the bath under equilibrium. Indeed, the order of the shifts corresponds to the order of the curves in Figure 1 copying their shape since the slopes (Table 2) are practically the same for all doses.

These results confirm our previous findings [32] on the dependence of atypical adsorption character of Cu(II) on wool on the absorbed dose, concentration and variability of the Cu-complexes.

Under the wool scouring, we used the chemical-free ultrasonic bath to avoid any effect of chemicals used in a standard scouring. We admit that an ultrasound impact may affect the development of the adsorption to some extent. As shown in Figure 2, the cortex scale of non-irradiated wool is not quite smooth unlike a standard scoured wool treated using detergents. Therefore, a slight wrinkling of the cortex is attributed to the ultrasound effect. The scale contours of the 48 kGy dosed fibre are less clear, as if more impaired. Although the difference is small, it is observable. The impaired spots could allow physical adsorption.

3.2 Testing of selected isotherm models and correlation data

To determine a suitable adsorption isotherm model for describing such unusual course of sorptivity, we tested the models summarized in Table 3. The performed sorption experiments provided data to calculate parameters necessary for individual isotherm models. Trend lines obtained for the graphs of the data calculated from the linearized equations (Table 3) are given in Table 4.

3.3 Data analysis

The correlation factor R^2 is generally considered to be the degree of conformation of the experimental data with the model. From the data in Table 4, it can be seen that in some cases the R^2 is more or less close to one and, in other cases, it is very far from it. To simplify the classification of data in Table 4, we pre-determined the boundary parameter of the correlation $R^2 \geq 0.91$ as fitting and $R^2 \langle 0.85-0.91 \rangle$ as quasi-fitting the given model, although several publications also calculate with $R^2 < 0.8$ [40].

Application of the pre-determined criteria showed that all tested samples fit only the Langmuir and Flory–Huggins models. As for the Redlich–Peterson model that matches the samples variably; it includes non-fitting, fitting and quasi-fitting cases (Table 4). Other models do not fit at all (the Dubinin–Radushkevich and Elovich) or only sporadically for the low doses (Freundlich, Temkin, Halsey, Harkins-Jura and Jovanovic quasi fit). More detailed data for the un-fitting models can be found in the Supplementary material.
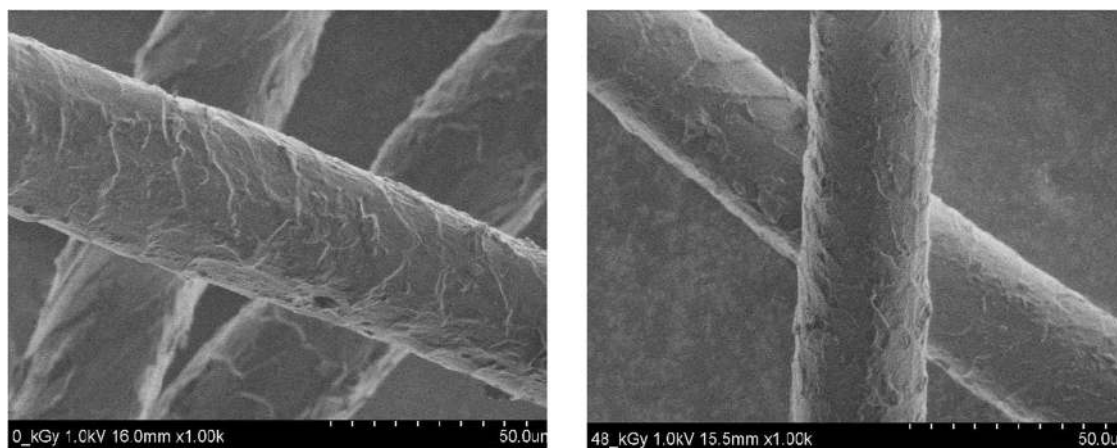

Figure 2: SEM images of the non-irradiated (left) and irradiated (right) fibres.

Table 3: Overview of the linearized equations of the tested isotherm models [37–39]

No.	Model	Linearized equation
1	Langmuir	$\frac{C_e}{q_e} = \frac{1}{Q \cdot K_L} + \frac{1}{Q} C_e$
2	Freundlich	$\log q_e = \log K_F + \frac{1}{n} \cdot \log C_e$
3	Dubinin–Radushkevich	$\ln q_e = \ln q_s - K_D \varepsilon^2; \varepsilon = RT \ln\left(1 + \frac{1}{C_e}\right)$
4	Temkin	$q_e = \frac{RT}{b} \ln K_T + \frac{RT}{b} \ln C_e$
5	Flory–Huggins	$\log\left(\frac{\theta}{C_0}\right) = \log K_{FH} + n \log(1 - \theta)$
6	Halsey	$\ln q_e = \frac{1}{n_H} \ln K_H - \frac{1}{n_H} \ln C_{q_e}$
7	Harkins-Jura	$\frac{1}{q_e^2} = \frac{B}{A} - \left(\frac{1}{A}\right) \log C_e$
8	Jovanovic	$\ln q_e = \ln q_{max} - K_J C_e$
9	Elovich	$\ln \frac{q_e}{C_e} = \ln K_E \cdot q_m - \frac{1}{q_m} q_e$
10	Redlich–Peterson	$\ln \frac{C_e}{q_e} = \beta \ln C_e - \ln A$

The Langmuir model is generally suitable for lower adsorbate concentrations, which is not quite well fulfilled in our case. As shown, the Cu(II) at a sufficient concentration very readily forms complexes with the ligands provided by keratin, immediately on the surface of the fibre [32]. Since the initial content of the carboxyl groups in keratin is higher than that of the amino groups [18], some parts of the complex molecule have to be ligands coming from several keratin chains, thus forming crosslinks. Such a network limits the entry of additional cations into the fibre volume, although electron beam irradiation creates potential conditions to form other complexes in the inner layers as well. The result is monolayer adsorption to which the Langmuir isotherm relates. However, homogeneity of the layer cannot be complete because the resulting S-oxidized species, especially cysteic acid, have to lead to different Cu-complexes. In addition, the electron beam disrupts the surface structure to some extent and can create pores. In such a case, the adsorption involves chemisorption with several variations of the mechanism, but in part also physical adsorption. Such opinion would correspond to the values of the correlation factor close to 1.

The Flory–Huggins model characterizes the degree of the surface coverage of the adsorbate and can express the feasibility and spontaneity of the adsorption [38]. As given in Table 4, all the systems adsorbent–adsorbate

Table 4: The correlation equations determined graphically for Cu(II) based on the linearized equations of models presented in Table 3

| Dose (kGy)	Trend link equation	Correlation	Trend link equation	Correlation
	Langmuir		**Flory–Huggins**	
0	$y = 0.0848x + 41.462$	$R^2 = 0.9172$	$y = -45.001x - 0.8894$	$R^2 = 0.9421$
20	$y = 0.0975x + 91.009$	$R^2 = 0.9259$	$y = -68.525x - 1.1024$	$R^2 = 0.9606$
24	$y = 0.0835x + 72.493$	$R^2 = 0.9822$	$y = -54.036x - 0.9791$	$R^2 = 0.9576$
48	$y = 0.1271x - 37.325$	$R^2 = 0.9276$	$y = -51.544x - 0.9889$	$R^2 = 0.9908$
100	$y = 0.1898x - 122.62$	$R^2 = 0.9177$	$y = -46.955x - 0.9733$	$R^2 = 0.9869$
165	$y = 0.1237x - 36.798$	$R^2 = 0.9578$	$y = -36.83x - 0.8315$	$R^2 = 0.9466$
	Redlich–Peterson			
0	$y = 0.892x - 0.4444$	$R^2 = 0.3876$		
20	$y = 0.6499x + 0.3393$	$R^2 = 0.9227$		
24	$y = 0.6918x + 0.1177$	$R^2 = 0.9841$		
48	$y = 0.8715x - 0.4864$	$R^2 = 0.9198$		
100	$y = 1.1433x - 1.3573$	$R^2 = 0.9067$		
165	$y = 1.0174x - 1.0312$	$R^2 = 0.8953$		
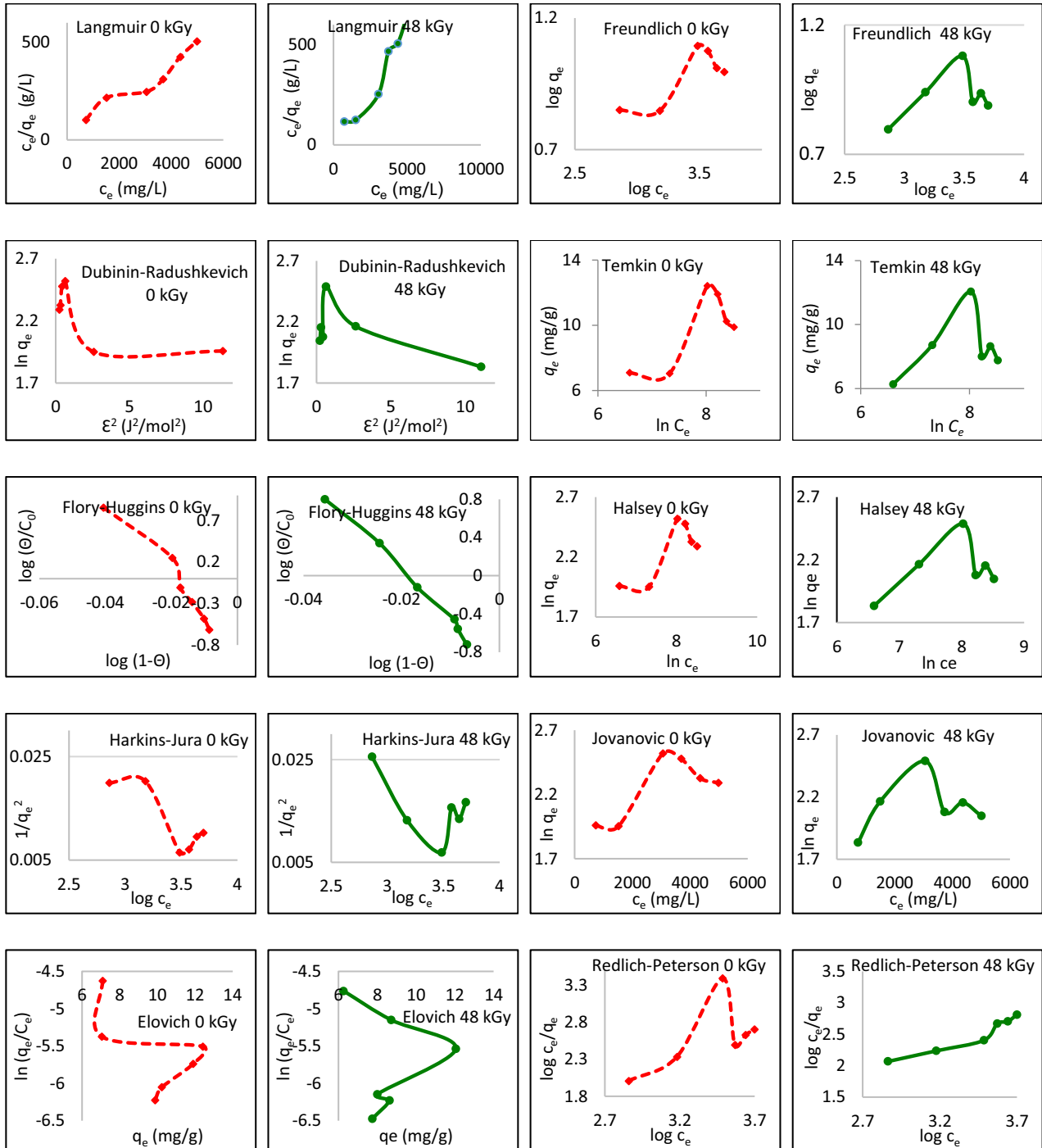
Figure 3: Selection of all tested adsorption models for Cu(II) sorption on the sheep wool dosed 0 and 48 kGy.

match the model fully showing evidence of the sorption process spontaneity. In addition, due to the variability of the Cu-complexes architecture [34–36], the adsorbate has the potential to cover the entire available surface. From all the models tested, the Flory–Huggins model shows the R^2 set values nearest to $R^2 = 1$ for all absorbed doses.

The Redlich–Peterson model is a hybrid isotherm mixing the Langmuir and Freundlich isotherms; therefore, it does not follow ideal monolayer adsorption [38]. In our case, various level of the fitting is observed. The non-irradiated wool is completely out of this hybrid model indicating a qualitative difference between both native and irradiated wool. The middle dosed wool samples of

20–48 kGy are fitting but, the highest doses of 100–165 kGy quasi fit only. Regarding the results obtained, the Redlich–Peterson model can be considered to be a dividing line to distinguish wool native ($R^2 = 0.3876$) from electron-modified ones ($R^2 \approx 0.9$), since the fitting Langmuir and Flory–Huggins models did not provide different data for wool native and modified.

Testing of the non-compliant models may result from their characteristics. The Freundlich model is not restricted to the formation of monolayer. It was usually applied to a heterogeneous surface and to multilayer adsorption even at higher concentrations. The Dubinin–Radushkevich as well as the Temkin model did not fit due to differentially distributed negative charge on the surface of natural sheep fibre [41], which is inconsistent with the assumption of both models. The Halsey and Harkin-Jura models were applied on multilayer adsorption at a relatively large distance from the surface and the adsorbent was heterogeneous with a heterogeneous distribution of pores [37]. Porous surface and the possibility of the adsorbate to bind physically related to the Jovanovic model in addition to the Langmuir model [42]. The Elovich model assumed an exponential growth of adsorption sites starting multilayer process [42], which is not our case. Although some results appear to be unnecessary, without any prior information on suitable isothermal models for the adsorbent–adsorbate systems under investigation, it would not be possible to classify the data.

3.4 Display of selected constructed plots

Reffering to Figure 2, Figure 3 demonstrates a condensed selection of the curves constructed for all linearized isotherm models for the samples dosed 0 and 48 kGy showing the impact of the irradiation on the quality of the fibre surface. Of course, every dose shows a distinct curve as indicated in Table 4 and the Supplementary materials.

3.5 Calculation of parameters for Cu-fitting and quasi-fitting models

The parameters calculated from the trend curves of the Langmuir, Flory–Huggins and Redlich–Peterson models are given in Table 5. Parameter Q in the Langmuir model represents the maximum amount of adsorbate per unit of adsorbent mass corresponding to complete coverage of adsorptive sites and the K_L is the Langmuir constant related to the energy of adsorption. If the highest values of the sorptivity (Figure 1) are approximately considered to be equivalent to Q, without optimization of the experimental conditions we observe a discrepancy between the experimental values and the calculated ones.

With some simplification and based on papers [32, 34–36], we can assume that the reasons are as follows: (a) double Cu(II)-salts (carboxylates and cysteinates) bound to different side branches of keratin chain, (b) several types of potential ligands (amines, imines, hydroxyls, sulfhydryls), (c) the ability of Cu(II) to form several geometric structures of the complexes, including degenerates depending on the ligand availability and the spatial possibilities on the surface and in subsurface layers of the fibre. Such combined circumstances can hardly be fully covered by a single model. A manifestation of this discrepancy may be a larger dispersion of the R^2 values.

In the Flory–Huggins model, the n_{FH} is the model exponent and the K_{FH} is an indication of the surface coverage degree at equilibrium. The K_{FH} is used to calculate of spontaneity free Gibbs energy. The ΔG^0 negative values in the Flory–Huggins isotherm confirm chemisorption (Table 5) even if the order of chemisorption intensity does not correspond to the sorptivity (Figure 1).

In the Redlich–Peterson model, the A is Redlich–Peterson constant and β is exponent in the basic (non-linearized) equation [38]. At high concentrations, the β tends to zero and approaches the Freundlich isotherm model while low concentrations give the β value close

Table 5: Parameters calculated for Cu-fitting and quasi-fitting[*] models for $T = 293$ K

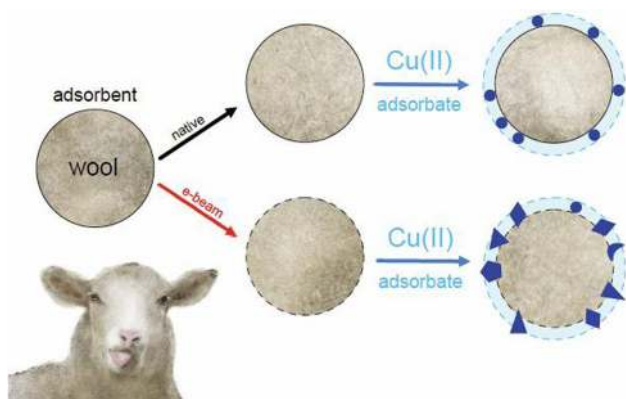| Dose	Langmuir		Flory–Huggins			Redlich–Peterson	
	$Q = 1/k$	K_L	K_{FH}	n_{FH}	$\Delta G^0 = RT \ln K_{FH}$	A	β
(kGy)	(mg/g)	(L/g)	(L/mol)		(kJ/mol)	(g/L)	
0	11.79	2.04	0.13	−45.00	−4.99	—	—
20	10.26	1.07	0.08	−68.52	−6.18	2.18	0.65
24	11.98	1.15	0.10	−54.04	−5.49	1.31	0.69
48	7.87	−3.40	0.10	−51.54	−5.55	0.33	0.87
100	5.27	−8.52	0.11	−46.95	−5.46	0.04	1.14
165	8.08	−3.36	0.15	−36.83	−4.66	0.09[*]	1.02[*]

Figure 4: Concept of mixed Cu(II) adsorption on electron irradiated sheep wool with the wool surface occupied with various Cu-complexes (chemisorption) along a minor contribution of physisorption.

to one indicating ideal Langmuir conditions [38,43]. As given in Table 5, the β in the Redlich–Peterson model for the irradiated samples approaches the Langmuir more than the Freundlich, although according to the above mentioned theory, the concentration conditions are just opposite in our case. Anyway, these facts support the opinion that Cu(II)-adsorption on the irradiated wool presents a hybrid model responsive to absorbed dose.

Figure 4 displays an assumed concept of such mixing sorption mechanism.

In light of the above-mentioned observations, the fluctuation of the sorptivity for wool-Cu(II) system (Figure 1) seems to be more understandable.

The subsequent work will be focused on the deposition of silver or other nanoparticles on such wool using a suitable colloidal system. One expected difficulty will be to identify the conditions under which the nanoparticles will have sufficient charge to maintain dispersion stability. Also stability of the whole system will be investigated. We believe that the new functionality of the irradiated wool could be useful for multiple applications.

Confrontation of our observations with results of other studies would be useful, however, at this time any similar data have not been published yet.

4 Conclusion

Radiation-modified wool studied in this work was proven to be an efficient adsorbent of Cu(II) redox cation from solution via chemisorption along a minor contribution of physisorption.

Among 10 tested adsorption models, only Langmuir, Flory–Huggins and partially Redlich–Peterson isotherms

showed fitting. Based on the completely different results for native wool from the radiation-modified ones, the Redlich–Peterson model is proposed as a distinguishing criterion between them. The next work is intended on the deposition of charged nanoparticles on the wool modified by an optimal absorbed dose and with redox metal adsorbed. Such study would be undertaken as part of the development of the method to provide new functionality to wool.

Conflict of interest: The authors declare no conflict of interest regarding the publication of this paper.

References

[1]   Hu P, Tan B, Long M. Advanced nanoarchitectures of carbon aerogels for multifunctional environmental applications. Nanotechnol Rev. 2016;5(1):23–39.

[2]   Li W, Zhao Y, Wang T. Study of Pb ion adsorption on (n, 0) CNTs (n = 4, 5, 6). Nanotechnol Rev. 2018;7(6):469–3.

[3]   Lin Y, Xu J, Sudhakar B, Gu J, Hong R. Preparation of spherical aminopropyl-functionalized MCM-41 and its application in removal of Pb(II) ion from aqueous solution. Nanotechnol Rev. 2019;8(1):275–4.

[4]   Reddy N, Zhou W, Ma M. Keratin-Based Materials. Berlin/Boston: Walter de Gruyter GmbH; 2020.

[5]   Kokot S. Sites for Cu(II) stabilization in Wool Keratin. Tex Res J. 1993;63(3):159–1.

[6]   Babincev LM, Budimir MV, Rajaković LV. Sorption of lead, cadmium and zinc from air sediments applying natural wool fiber. Sorpcija olova, kadmijuma i cinka iz sedimenata iz vazduha primenom vlakana prirodne vune. Hem Ind. 2013;67(2): 349–5.

[7]   Wen G, Naik R, Cookson PG, Smith SV, Liu X, Wang XG. Wool powders used as sorbents to remove Co^{2+} ions from aqueous solution. Powder Technol. 2010;197(3):235–0.

[8]   Atef El-Sayed A, Salama M, Kantouch AAM. Wool micro powder as a metal ion exchanger for the removal of copper and zinc. Desalin Water Treat. 2015;56(4):1010–9.

[9] Balkaya N, Bektasb N. Chromium(VI) sorption from dilute aqueous solutions using wool. Desalin Water Treat. 2009;3(1–3):43–9.

[10] Manassra A, Khamis M, Ihmied T, Eldakiky M. Removal of chromium by continuous flow using wool packed columns. Elec J Env Agric Food Chem. 2010;9(3):651–3.

[11] Jumean F, Khamis M, Sara Z. Concurrent removal and reduction of Cr(VI) by wool: short and long term equilibration studies. Am J Anal Chem. 2015;6(1):47–7.

[12] Ray P, Sabri M, Ibrahim H, Khamis MI, Jumean FH. Design and optimization of a batch sequential contactor for the removal of chromium(VI) from industrial wastewater using sheep wool as low cost adsorbent. Desalin Water Treat. 2018;113:109–3.

[13] Mažeikiene A, Vaiškunaite R, Vaišis V. Oil removal from runoff with natural sorbing filter fillers. J Env Manage. 2014;141:155–0.

[14] Rajakovic V, Aleksic G, Radetic M, Rajakovic Lj. Efficiency of oil removal from real wastewater with different sorbent materials. J Hazard Mater. 2007;143(1–2):494–9.

[15] Cieślak M, Schmidt H. Contamination of wool fibre exposed to environmental tobacco smoke. Fibres Text East Eur. 2004;2(1):81–3.

[16] Curling SF, Loxton C, Ormondroyd GA. A Rapid method for investigation the absorption of formaldehyde from air by wool. J Mater Sci. 2012;47(7):3248–1.

[17] Taddei P, Monti P, Freddi G, Arai T, Tsukada M. Binding of Co(II) and Cu(II) cations to chemically modified wool fibres. An IR investigation. J Mol Struct. 2003;650(1–3):105–3.

[18] Nikiforova TE, Kozlov VA, Sionikhina AN. Peculiarities of sorption of copper(II) ions by modified wool keratin. Prot Met Phys Chem. 2019;55:849–7.

[19] Abdel Ghafar HH, Salem T, Radwan EK, Atef El-Sayed A, Embaby M. Modification of waste wool fiber as low cost adsorbent for the removal of methylene blue from aqueous solution. Egypt J Chem. 2017;60(3):395–6.

[20] Kan CW, Yuen CWM. Plasma technology in wool. Tex Prog. 2007;39(3):121–87.

[21] Fakin D, Ojstršek A, Čelan, Benkovič S. The impact of corona modifies fibres´chemical changes on wool dyening. J Mater Process Technol. 2009;209(1):584–9.

[22] Ke G, Yu W, Xu W, Cui W, Shen X. Effect of corona discharge treatment on the surface properties of wool fabrics. J Mater Process Technol. 2008;207(1–3):125–9.

[23] Perumalraj R. Effect of silver nanoparticles on wool fibre. ISRN Chem Eng. 2012; Article ID 842021, 4 pages.

[24] Chattopadhyay DP, Patel BH. Improvement in physical and dyeing properties of natural fibres through pre-treatment with silver nanoparticles. Indian J Fibre Text Res. 2009;34:368–3.

[25] Gokarneshan N. A review of some significant insights on nano finishing of protein fibres. J Nanosci Nanotechnol Res. 2018;2(1):4.

[26] Porubská M, Hanzlíková Z, Braniša J, Kleinová A, Hybler P, Fülöp M, et al. The effect of electron beam on sheep wool. Polym Degrad Stab. 2015;111:151–8.

[27] Hanzlíková Z, Lawson MK, Hybler P, Fülöp M, Porubská M. Time-dependent variations in structure of sheep wool irradiated by electron beam. Adv Mater Sci Eng. 2017; Article ID 3849648, 10 pages.

[28] Hanzlíková Z, Braniša J, Hybler P, Šprinclová I, Jomová K, Porubská M. Sorption properties of sheep wool irradiated by accelerated electron beam. Chem Pap. 2016;70:1299–8.

[29] Hanzlíková Z, Braniša J, Jomová K, Fülöp M, Hybler P, Porubská M. Electron beam irradiated sheep wool – Prospective sorbent for heavy metals in wastewater. Sep Purif Technol. 2018;193:345–0.

[30] Braniša J, Kleinová A, Jomová K, Malá R, Morgunov V, Porubská M. Some properties of electron beam-irradiated sheep wool linked to Cr(III) sorption. Molecules. 2019;24(24):15.

[31] King DG, Pierlot AP. Absorption of nanoparticles by wool. Color Technol. 2009;125:111–6.

[32] Porubská M, Kleinová A, Hybler P, Braniša J. Why natural or electron irradiated sheep wool show anomalous sorption of higher concentrations of copper(II). Molecules. 2018;23:15.

[33] González-Hurtado M, Marins JA, Guenther Soares B, Rieumont Briones J, Rodríguez Rodríguez A, Ortiz-Islas E. Magnetic SiO₂-Fe₃O₄ nanocomposites as carriers of ibuprofen for controlled release applications. Rev Adv Mater Sci. 2018;55:12–20.

[34] Baryshnikova AT, Minaev BF, Baryshnikov GV, Sun WH. Quantum-chemical study of the structure and magnetic properties of mono- and binuclear Cu(II) complexes with 1,3-bis(3-(pyrimidin-2-yl)-1*H*,-1,2,4-triazol-5-yl)propane. Russ J Inorg Chem. 2016;61:588–3.

[35] Baryshnikov GV, Minaev BF, Baryshnikova AT, Ågren H. Anion-induced exchange interactions in binuclear complexes of Cu(II) with flexible hexadentate bispicolylamidrazone ligands. Chem Phys Lett. 2016;661:48–2.

[36] Baryshnikova AT, Minaev BF, Baryshnikov GV, Ågren H. A computational study of the structure and magnetic properties of the weakly coupled tetranuclear square-planar complex of Cu(II) with a tetraporphyrin sheet. Inorganica Chim Acta. 2019;485:73–9.

[37] Amin MT, Alazba A, Shafiq M. Adsorptive removal of reactive Black 5 from wastewater using bentonite clay: isotherms, kinetics and thermodynamics. Sustainability. 2015;7(11):15302–8.

[38] Foo KY, Hameed BH. Insights into the modeling of adsorption isotherm systems. Chem Eng J. 2010;156(1):2–10.

[39] Hamdaoui O, Naffrechoux E. Modeling od adsorption isotherms of phenol and chlorophenols onto granular activated carbon. Part I. Two-parameter models and equations allowing determination of thermodynamic parameters. J Hazard Mater. 2007;147(1–2):381–4.

[40] Kilpimaa S, Runtti H, Kangas T, Lassi U, Kuokkanen T. Physical activation of carbon residue from biomass gasification: novel sorbent for the removal of phosphates and nitrates from aqueous. J Ind Eng Chem. 2015;21:1354–4.

[41] Zimmerman B, Chow J, Abbott AG, Ellison MS, Kennedy MS, Dean D. Variation of surface charge along the surface of wool fibers assessed by high-resolution force spectroscopy. J Eng Fiber Fabr. 2011;6(2):61–6.

[42] Farouq R, Yousef NS. Equilibrium and kinetics studies of adsorption of copper(II) ions on natural biosorbent. Int J Chem Eng Appl. 2015;6(5):319–4.

[43] Jossens L, Prausnitz JM, Fritz W, Schlünder EU, Myers AL. Thermodynamics of multi-solute adsorption from dilute aqueous solutions. Chem Eng Sci. 1978;33(8):1097–6.